

Stripelike magnetism in a mixed-valence insulating state of the Fe-based ladder compound CsFe_2Se_3

Fei Du,^{1,2} Kenya Ohgushi,^{1,3} Yusuke Nambu,^{3,4} Takateru Kawakami,⁵ Maxim Avdeev,⁶ Yasuyuki Hirata,¹ Yoshitaka Watanabe,⁵ Taku J Sato,^{3,4,7} and Yutaka Ueda^{1,3}

¹*Institute for Solid State Physics, University of Tokyo, Kashiwanoha, Kashiwa, Chiba 277-8581, Japan*

²*Key Laboratory of Physics and Technology for Advanced Batteries (Ministry of Education), College of Physics, Jilin University, Changchun 130012, People's Republic of China*

³*JST, TRIP, 5 Sanbancho, Chiyoda, Tokyo 102-0075, Japan*

⁴*Neutron Science Laboratory, Institute for Solid State Physics, University of Tokyo, Tokai, Ibaraki 319-1106, Japan*

⁵*Institute of Quantum Science, Nihon University, Chiyoda, Tokyo 101-8308, Japan*

⁶*Bragg Institute, Australian Nuclear Science and Technology Organization, PMB1, Menai, NSW 2234, Australia*

⁷*Institute of Multidisciplinary Research for Advanced Materials, Tohoku University, Katahira 2-1-1, Sendai 980-8577, Japan*

(Received 10 April 2012; revised manuscript received 31 May 2012; published 28 June 2012)

Structural and electronic properties of the Fe-based spin-ladder compound CsFe_2Se_3 was investigated by means of resistivity, susceptibility, specific heat, Mössbauer, and neutron diffraction measurements. Despite the single-site nature in a mixed-valence state, the ground state is a magnetic insulator characterized by a charge gap ~ 0.34 eV and an antiferromagnetic transition temperature 175 K. The magnetic structure was stripelike, with magnetic moments of $1.77(6)\mu_B$ coupled ferromagnetically (antiferromagnetically) along the rung (leg) direction. Both the insulating behavior and stripelike ordering can be understood by assuming extra carriers delocalized on the rung. Our findings reveal that CsFe_2Se_3 is an appealing compound with the stripelike magnetic structure in an insulating state among Fe-based compounds, and provide significant supplemental insight into the magnetism of Fe-based superconductors.

DOI: 10.1103/PhysRevB.85.214436

PACS number(s): 72.20.-i, 75.25.-j, 75.40.-s, 75.50.Ee

I. INTRODUCTION

Motivated by the discovery of Fe-based superconductors (SC), research on the interplay between crystal structure, magnetism, and superconductivity has become a main stream in condensed-matter physics.^{1–3} The basic structural feature connecting these Fe-based compounds is the presence of square planar sheets of Fe atoms coordinated tetrahedrally by pnictogens or chalcogens. The most common magnetic structure is a striped order including both single-stripe and double-stripe types; the microscopic mechanism of this stripe order has been under intense debate between the localized versus itinerant pictures.^{4–8} More recently, block magnetism was found in $A_2\text{Fe}_4\text{Se}_5$ ($A = \text{K}$, Rb , and Cs), and has been considered the second type of magnetic structure.⁹ To gain further insight into the mechanism and variation of magnetic order, investigation of Fe-based compounds with various dimensions is important, because the dimensionality strongly influences not only the spin network but also the itinerancy of electrons through the change in the Fermi-surface topology.

Recently, the quasi-one-dimensional spin-ladder compound BaFe_2Se_3 has attracted considerable attention.^{10–13} A neutron diffraction study revealed that local atomic displacement triggers a magnetic transition from short-range antiferromagnetic (AFM) correlation to long-range AFM ordering at 255 K. The magnetic moments of $2.8\mu_B$ are arranged to form an Fe_4 ferromagnetic (FM) unit, and each FM unit stacks antiferromagnetically along the leg direction;^{10,11} this is a one-dimensional analog of the block magnetism. CsFe_2Se_3 , which crystallizes in the orthorhombic space group $Cmcm$,¹⁴ is another prominent example with the same structural motif as BaFe_2Se_3 . The structure can also be described as double chains of $[\text{Fe}_2\text{Se}_3]^{1-}$ formed by edge-shared FeSe_4 tetrahedra extending along the c axis, with channels occupied by Cs

atoms, as shown in Fig. 1(a). One important feature is the mixed-valence state; the formal valence of Fe ions is 2.5 in contrast to the ferrous character in BaFe_2Se_3 . Hence, one would expect a metallic state and hopefully a superconducting state, as in the case of KFe_2As_2 .¹⁵

Here, we present a study on the electronic properties of the Fe-based spin-ladder compound CsFe_2Se_3 . We show that the compound is an insulator and undergoes a transition into a stripelike AFM order at 175 K, and discuss the electronic state with a special focus on extra carriers inherent in the mixed-valence state.

II. EXPERIMENT

Single crystalline CsFe_2Se_3 was synthesized by the slow cooling method. Starting materials with a nominal composition of $\text{Cs}_2\text{Se}:\text{Fe}:\text{Se} = 1:4:5$ were mixed and placed into an alumina crucible, then sealed in a double quartz tube under 0.3 atm of Ar. The quartz tube was annealed at 949 °C for 24 h and slowly cooled to 650 °C at approximately 3 °C/h. A typical needlelike single crystal nearly 5 mm in length was obtained. The chemical composition was determined to be stoichiometric by an energy-dispersive x-ray spectrometer. The electrical resistivity, susceptibility, and specific heat were measured using a commercial setup (Quantum Design). Mössbauer measurements down to 10 K were performed for crushed crystals using a γ -ray source of ^{57}Co in Rh matrixes of 925 MBq with active areas 5 mm in diameter. The velocity scale of the spectra was relative to that of α -Fe at room temperature. Neutron powder diffraction data were collected on the high-resolution ECHIDNA diffractometer at ANSTO with $\lambda = 2.4395$ Å. Diffraction patterns were obtained between 3 and 350 K in a closed-cycle refrigerator.

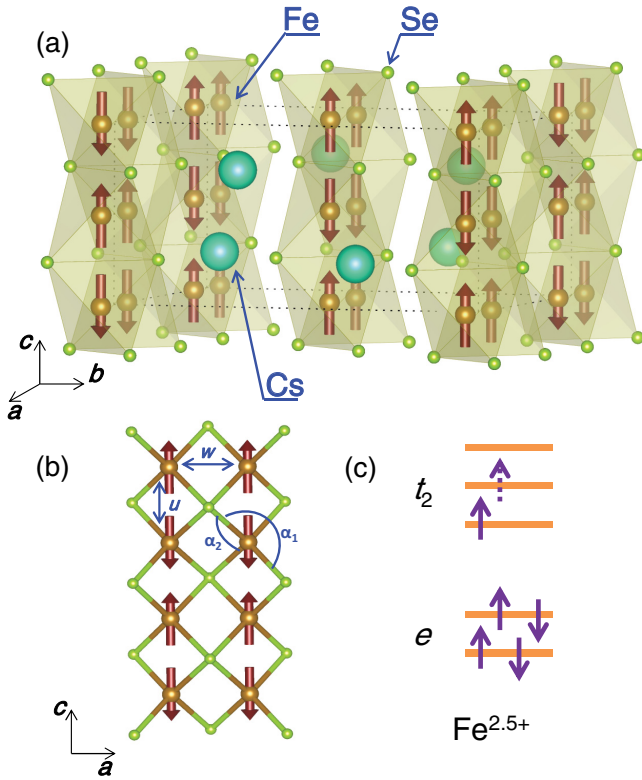


FIG. 1. (Color online) (a) Crystal and magnetic structures of CsFe_2Se_3 . A cuboid with dashed lines indicates a crystallographic unit cell; (b) the magnetic structure in a ladder; and (c) a proposed electronic configuration of $\text{Fe}^{2.5+}$ ions.

III. RESULTS AND DISCUSSION

Table I summarizes the structural parameters at 300 K determined by Rietveld refinement of powder neutron diffraction data (data not shown). Consistent with an earlier report,¹⁴ the crystal structure is well accounted for by an orthorhombic space group $Cmcm$. The temperature (T) dependence of the lattice parameters is provided in Fig. 2(a), indicating a systematic change with no sign of a structural transition.

The temperature dependence of the resistivity ρ along the c axis indicates an insulating behavior in the measured T region [Fig. 2(b)]. The room- T value is $8.8 \times 10^3 \Omega \text{ cm}$, which is nearly three orders of magnitude larger than that of the spin-ladder analog BaFe_2Se_3 ($17 \Omega \text{ cm}$).¹² Fitting to the thermal activation formula $\rho = \rho_0 \exp(E_a/k_B T)$, where ρ_0 is a prefactor and k_B is the Boltzmann's constant, yielded the thermal activation energy $E_a = 0.34 \text{ eV}$. This value is also

TABLE I. Atomic positions at $T = 300 \text{ K}$ determined by Rietveld analysis for CsFe_2Se_3 with a $Cmcm$ space group. Lattice constants are $a = 9.8426(2) \text{ \AA}$, $b = 11.8297(3) \text{ \AA}$, and $c = 5.6904(1) \text{ \AA}$. An isotropic Debye-Waller factor (U_{iso}) was employed.

| Atom | Site | x | y | z | $U_{\text{iso}} (\text{\AA}^2)$ |
|------|------|-----------|-----------|-----|---------------------------------|
| Cs | 4c | 1/2 | 0.1618(5) | 1/4 | 0.025(2) |
| Fe | 8e | 0.3601(3) | 1/2 | 0 | 0.015(1) |
| Se1 | 4c | 0 | 0.1223(4) | 1/4 | 0.025(2) |
| Se2 | 8g | 0.2272(3) | 0.3882(3) | 1/4 | 0.021(1) |

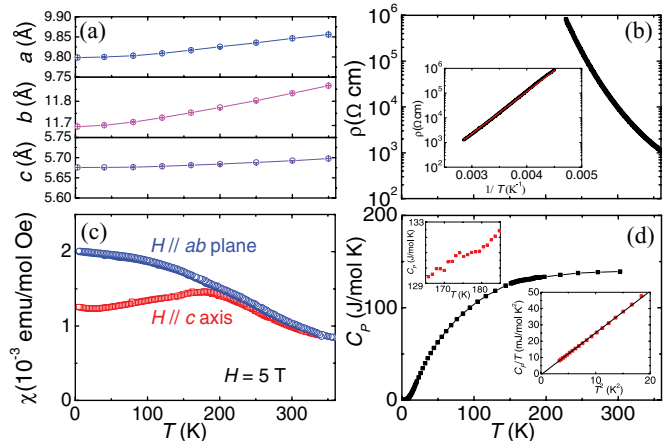


FIG. 2. (Color online) Temperature (T) dependences of (a) lattice parameters; (b) electrical resistivity (ρ); (c) magnetic susceptibility (χ) along the c axis and the ab plane in a magnetic field (H) of 5 T under the zero-field-cooled (closed circle) and field-cooled (open circle) conditions; and (d) specific heat (C_p). The inset of (b) shows a fit of ρ with a thermal activation model. The left and right insets of (d) indicate a magnified view of C_p near the magnetic transition T and results of cubic term fit, respectively.

larger than that of BaFe_2Se_3 (0.18 eV).¹² This more insulating behavior in a mixed-valence state was unexpected, and the causes will be discussed below.

The magnetic susceptibility χ under a magnetic field of 5 T applied along and perpendicular to the c axis is shown in Fig. 2(c). At high T , the susceptibility increases with decreasing T , but detailed analysis is impossible owing to a small amount of ferromagnetic impurity phases. On further cooling, the χ along the c axis shows a rapid decrease below $\sim 175 \text{ K}$, whereas the χ within the ab plane increases continuously. These features correspond to the magnetic transition into AFM order with spins oriented along the c axis; this is consistent with the magnetic structure based on the neutron diffraction analysis (see the discussion below).

The specific heat C_p shows no λ -type anomaly near the Néel temperature T_N [Fig. 2(d)], suggesting that the entropy release associated with the magnetic ordering occurs gradually in a low-dimensional system. At low T , C_p can be fitted solely by a cubic term βT^3 [right inset of Fig. 2(d)]. The lack of the γT term is in agreement with the insulating nature. From $\beta = 2.63 \text{ mJ/mol K}^4$, the Debye temperature θ_D was estimated to be 164 K using the formula $\beta = 12\pi^4 N R / 5\theta_D^3$ (N is the number of atoms in a formula unit, 6, and R is the gas constant).

The temperature dependence of the Mössbauer spectra is shown in Fig. 3 and the analyzed Mössbauer parameters are displayed in Fig. 4. At room T , the spectra are quadrupole split paramagnetic lines and can be well fit with one doublet. Putting the isomer shift value $IS = 0.39(1) \text{ mm/s}$ at 298 K into an empirical formula $IS = 1.68 - 0.5\langle m \rangle$,¹⁶ we can estimate the mean valence $\langle m \rangle$ to be 2.58, which indicates that the local environment and Fe valence are unique, ruling out a spatial distribution of $\text{Fe}^{2+}/\text{Fe}^{3+}$ ions (the charge-ordered state). Below 170 K, a magnetically split sextet appears in addition to a doublet component and this sextet gradually increases in weight with decreasing T . It should be noted that

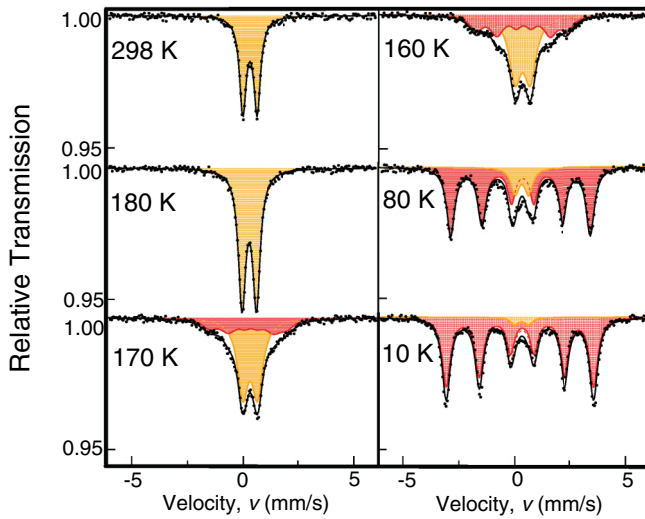


FIG. 3. (Color online) ^{57}Fe Mössbauer spectra of CsFe_2Se_3 obtained at various temperatures.

the signature of charge ordering was still absent below T_N . The coexistence of paramagnetic/antiferromagnetic phases, which has also been found in $\text{Rb}_{0.8}\text{Fe}_{1.6}\text{Se}_2$,¹⁷ remained at the lowest T measured, supporting the gradual formation of a magnetic ground state indicated by the lack of any observed anomaly in C_p at T_N . The magnetic hyperfine field with saturation value is 20.7 T at 10 K. The quadrupole splitting (QS), which is a measure of local electric field gradient produced by nonspherical charge distribution, dramatically changes from 0.62 to -0.08 mm/s across the magnetic transition [Fig. 4(b)].

This single-site nature even in the mixed-valence state seems to be incompatible with the insulating behavior. However, this can be reconciled by assuming that extra electrons inherent in the mixed-valence state are equally occupied by two Fe spins on a rung, but do not conduct along the leg direction. The conduction is governed by the overlapping of Fe 3d orbitals along the leg direction;^{12,18} the longer Fe-Fe bond distances along the leg direction, $u = 2.85$ Å in CsFe_2Se_3 vs $u = 2.72$ Å in BaFe_2Se_3 , is consistent with the more localized nature of CsFe_2Se_3 . Therefore, it is likely that CsFe_2Se_3 would become a metal or superconductor by shortening the leg distance under chemical or physical pressure.

In order to obtain more information on this microscopic magnetism, high-resolution powder neutron diffraction was performed. Figure 5 shows a diffraction pattern taken at 3 K along with Rietveld refinement results obtained using FullProf.¹⁹ All magnetic peak positions can be indexed by a propagation wave vector, $\mathbf{q}_m = (1/2, 1/2, 0)$. To identify the magnetic structure, we applied representation analysis. Basis vectors (BVs) of the irreducible representations (irreps) of the wave vector were obtained using the SARAH code (Table II).²⁰ There are four irreps, and each rep consists of three BVs describing the collinearity of magnetic moments along one crystallographic axis. First, we sorted all BVs by comparing R factors and found that ψ_9 has the best fit, with $R_{\text{mag}} = 9.42\%$. Next, we tested the potential involvement of ψ_7 and ψ_8 , which both belong to the same rep as ψ_9 , Γ_3 . However, this did not improve the fitting quality; this is consistent with the susceptibility results suggesting Ising-like spins along the

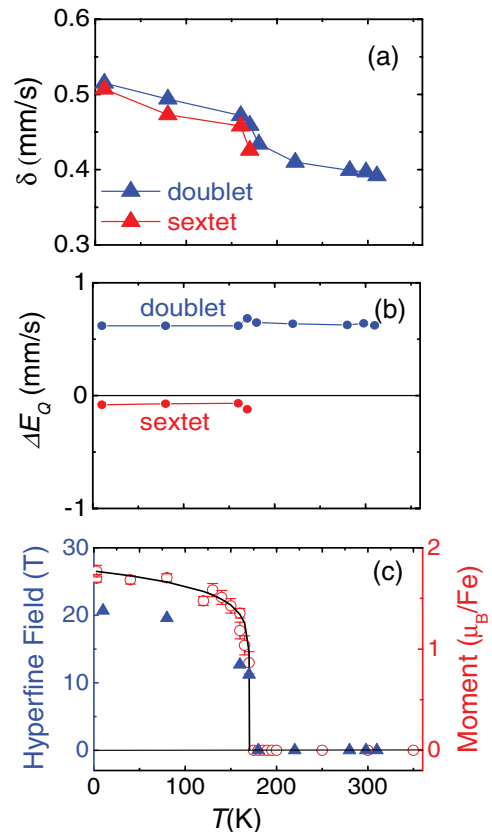


FIG. 4. (Color online) Temperature (T) dependences of (a) isomer shift (δ); (b) quadrupole splitting (ΔE_Q) of doublet and sextet components; and (c) hyperfine field deduced from the Mössbauer spectra and the estimated magnetic moment from the neutron diffraction profile. The solid line is a guide for the eyes.

c axis. The obtained magnetic structure is shown in Figs. 1(a) and 1(b). Magnetic moments are arranged to form a FM unit along the rung direction (the a axis), and FM units are stacked antiferromagnetically along the leg direction (the c axis). For interladder coupling on the ab plane, a unit of

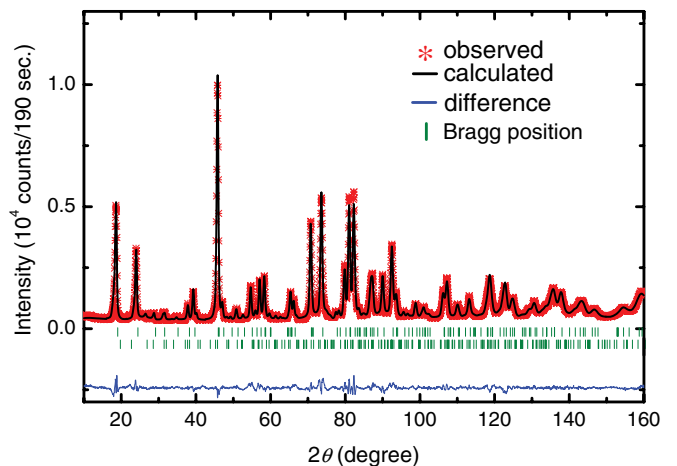


FIG. 5. (Color online) Neutron powder diffraction pattern of CsFe_2Se_3 at 3 K with Rietveld refinement results (solid lines). The bottom line shows the difference between observed and calculated intensities.

TABLE II. Basis vectors (BVs) of irreducible representations (irreps) for the space group $Cmcm$ with the magnetic wave vector $\mathbf{q}_m = (1/2, 1/2, 0)$. Superscripts show the moment direction. Columns for position represent No. 1: $(x, 1/2, 0)$, No. 2: $(-x + 1, 1/2, 1/2)$, No. 3: $(-x + 1, 1/2, 0)$, and No. 4: $(x, 1/2, 1/2)$.

| Irrep | BV | No. 1 | No. 2 | No. 3 | No. 4 |
|------------|-------------|-------|--------|--------|--------|
| Γ_1 | ψ_1 | 1^a | -1^a | 1^a | -1^a |
| | ψ_2 | 1^b | -1^b | 1^b | -1^b |
| | ψ_3 | 1^c | 1^c | 1^c | 1^c |
| Γ_2 | ψ_4 | 1^a | -1^a | -1^a | 1^a |
| | ψ_5 | 1^b | -1^b | -1^b | 1^b |
| | ψ_6 | 1^c | 1^c | -1^c | -1^c |
| Γ_3 | ψ_7 | 1^a | 1^a | 1^a | 1^a |
| | ψ_8 | 1^b | 1^b | 1^b | 1^b |
| | ψ_9 | 1^c | -1^c | 1^c | -1^c |
| Γ_4 | ψ_{10} | 1^a | 1^a | -1^a | -1^a |
| | ψ_{11} | 1^b | 1^b | -1^b | -1^b |
| | ψ_{12} | 1^c | -1^c | -1^c | 1^c |

FM spins correlates antiferromagnetically in one neighboring ladder and ferromagnetically in the perpendicular direction; this sequence of interladder couplings is the same as in BaFe_2Se_3 . The determined magnetic structure, which is similar to a “single stripe,” is reminiscent of 1111, 122, and 111 systems and is consistent with a recent study of KFe_2Se_3 .²¹ The estimated moment at 3 K is $1.77(6) \mu_B/\text{Fe}$. The temperature dependence of the determined magnetic moment shown in Fig. 4(c) scales well with the hyperfine field obtained from Mössbauer measurements.

Despite the diversity in crystal structure and chemical composition, two types of magnetic structures have been reported to date in Fe-based SCs: stripe magnetism (single- and double-stripe) in 1111, 122, 111, and 11 systems,^{1–3} and the more recent block magnetism in $\text{K}_2\text{Fe}_4\text{Se}_5$.^{9,22} In a ladder structure, block magnetism in BaFe_2Se_3 has been observed.^{10,11} Our finding of stripe magnetism in CsFe_2Se_3 , which shows a stripelike order in an insulating state, provides a missing link, and implies that the underlying mechanism of magnetic properties has a common origin, irrespective of crystal structure. This is further supported by the interesting observation that, in both square and ladder structures, spins are oriented in the square/ladder planes in striped magnetism and perpendicular to the square/ladder planes in block magnetism.

In Fe-based SCs, magnetic structure shows a close correlation with the ordered moment: single-stripe magnetism usually has an ordered moment smaller than $1\mu_B$, whereas block magnetism has a larger moment around $3\mu_B$. The observed moment of $1.8\mu_B$ in CsFe_2Se_3 and $2.8\mu_B$ in BaFe_2Se_3 ¹⁰ is qualitatively consistent with this correlation; however, quantitatively, the magnetic moment of CsFe_2Se_3 is the largest among known single-stripe magnetism. This is most likely associated with the insulating nature in contrast to the metallic state of the parent compounds of Fe-based SCs. Within the localized model, the average theoretically expected moment for the high spin state of Fe^{2+} and Fe^{3+} ions is $4.5\mu_B$, which is much larger than the observed value. Instead, the intermediate spin state, where the e bands are fully occupied and the t_2 bands are partially occupied, would lead to a magnetic moment of

$1.5\mu_B$ for $\text{Fe}^{2.5+}$ ions [Fig. 1(c)]; if we further assume partial hole doping into the e bands, the observed magnetic moment is well accounted for.

There is a continuing controversy regarding whether stripe magnetism in Fe-based SCs is best described by the localized model or the itinerant picture.^{1,2,23,24} Considering the insulating behavior, we should first adopt the localized model for CsFe_2Se_3 . The competing exchange interaction between the nearest-neighbor (NN) and next-nearest-neighbor (NNN) Fe ions is expected to induce stripelike ordering when $J_1 < 2J_2$, where J_1 and J_2 denote the AFM exchange coupling between NN and NNN Fe atoms, respectively.^{25,26} However, it is difficult to understand the fairly high T_N from a magnetic frustration aspect. There should be a factor which differentiates the NN exchange interactions along the leg direction from those along the rung direction.

The most plausible scenario is that the extra electrons delocalized on the rung play an important role. If the extra electrons hopping quickly along the rung direction prefer to be parallel to the spin at the Fe site because of the local Hund coupling, these electrons would mediate a ferromagnetic interaction between two Fe spins (double exchange mechanism). A stripelike order with a fairly high T_N would thus be realized. This idea is corroborated by reported results for AgFe_2S_3 , which is another mixed-valence insulator with an $\text{Fe}^{2.5+}$ state. In this compound, Fe tetrahedra form a zigzag chain by sharing edges with alternating bond lengths.²⁷ The magnetic structure is an up-up-down-down type as a consequence of ferromagnetic (antiferromagnetic) coupling of shorter (longer) Fe-Fe bonds. It was discussed that this magnetic structure is stabilized by the delocalized extra electrons within the shorter Fe-Fe bonds. In CsFe_2Se_3 , the bond distance between NN Fe atoms along the rung direction ($w = 2.75 \text{ \AA}$) is shorter than that along the leg direction ($u = 2.85 \text{ \AA}$). Through consideration of both the location of extra carriers and the exchange interaction for AgFe_2S_3 , the observed stripelike magnetism can be well understood. An interesting possibility is that ferro-type orbital ordering of, e.g., xy bands reinforces the ferromagnetic interaction along the rung as discussed in Fe-based SCs.^{8,28,29} This likely happens in CsFe_2Se_3 , as suggested by the dramatic change in QS upon magnetic ordering [Fig. 4(b)]; however, further studies are needed to confirm this.

IV. SUMMARY

Our results reveal an insulating behavior with the lack of charge order, and the stripelike magnetic order at 175 K in the spin-ladder compound CsFe_2Se_3 . The stripe order in an insulating state among Fe-based compounds indicates that a simple itinerant picture based on Fermi-surface nesting is invalid as an origin. Indeed, our results demonstrated that the single-stripe magnetic structure is stabilized by an intimate coupling among spin, charge, and possibly orbital degrees of freedom.

ACKNOWLEDGMENTS

We thank M. Isobe, K. Asoh, and H. Matsuda for technical assistance. This work was supported by Special Coordination Funds for Promoting Science and Technology “Promotion of Environmental Improvement for Independence of Young Researchers,” and Grant-in-Aid for Scientific Research (Grant

No. 23340097). F.D. would like thank the National Natural Science Foundation of China (Grant No. 11004073).

APPENDIX

A local distortion coupled with magnetic ordering was observed in BaFe_2Se_3 .¹⁰ In order to detect possible magnetoelastic coupling and Fe displacement in CsFe_2Se_3 , we examined the local crystal structure on the basis of the neutron diffraction measurements. As shown in Fig. 6, the ratio of bond distance between nearest-neighbor Fe-Fe ions along the rung direction (w) and leg direction (u), the Fe ion position, and the bond angle of Se-Fe-Se in FeSe_4 tetrahedra are nearly temperature independent. Similar behavior has been observed in KFe_2Se_3 , which exhibits the same striped ordering.²¹ These results indicate that the striped ordering with spins oriented along the leg direction is not stabilized by magnetoelastic coupling.

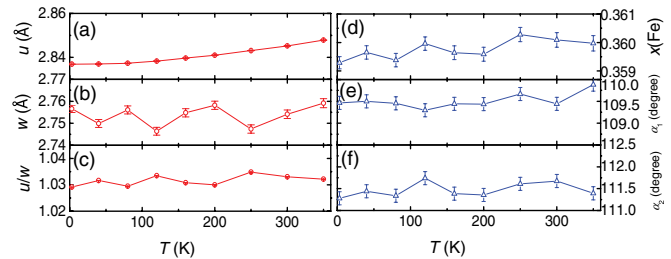


FIG. 6. (Color online) Temperature (T) dependence of (a) bond length along the leg (u) and (b) rung (w) direction; (c) ratio between bond length along the leg and rung direction; (d) x parameter of the Fe site; and (e) and (f) Se-Fe-Se bond angle α_1 and α_2 [see Fig. 1(b)].

We note that this conclusion is compatible with the orbital ordering of electronic origin, which need not accompany large structural distortions.

¹M. D. Lumsden and A. D. Christianson, *J. Phys: Condens. Matter* **22**, 203203 (2010).
²G. R. Stewart, *Rev. Mod. Phys.* **83**, 1589 (2011).
³D. J. Singh, *Physica C* **469**, 418 (2009).
⁴P. Hansmann, R. Arita, A. Toschi, S. Sakai, G. Sangiovanni, and K. Held, *Phys. Rev. Lett.* **104**, 197002 (2010).
⁵S. A. J. Kimber, A. Kreyssig, Y. Z. Zhang, H. O. Jeschke, R. Valenti, F. Yokochihiya, E. Colombier, J. Q. Yan, T. C. Hansen, T. Chatterji, R. J. McQueeney, P. C. Canfield, A. I. Goldman, and G. N. Argyriou, *Nature Mater.* **8**, 471 (2009).
⁶T. Yildirim, *Phys. Rev. Lett.* **101**, 057010 (2008).
⁷Q. M. Si and E. Abrahams, *Phys. Rev. Lett.* **101**, 076401 (2008).
⁸C. C. Lee, W. G. Yin, and W. Ku, *Phys. Rev. Lett.* **103**, 267001 (2009).
⁹M. Y. Wang, C. Fang, D. X. Yao, G. T. Tan, L. W. Harriger, Y. Song, T. Netherton, C. L. Zhang, M. Wang, M. B. Stone, W. Tian, J. P. Hu, and P. C. Dai, *Nat. Commun.* **2**, 580 (2011).
¹⁰Y. Nambu, K. Ohgushi, S. Suzuki, F. Du, M. Avdeev, Y. Uwatoko, K. Munakata, H. Fukazawa, S. X. Chi, Y. Ueda, and T. J. Sato, *Phys. Rev. B* **85**, 064413 (2012).
¹¹J. M. Caron, J. R. Neilson, D. C. Miller, A. Llobet, and T. M. McQueen, *Phys. Rev. B* **84**, 180409(R) (2011).
¹²H. C. Lei, H. Ryu, A. I. Frenkel, and C. Petrovic, *Phys. Rev. B* **84**, 214511 (2011).
¹³B. Saparov, S. Calder, B. Sipos, H. Cao, S. Chi, D. J. Singh, A. D. Christianson, M. D. Lumsden, and A. S. Sefat, *Phys. Rev. B* **84**, 245132 (2011).
¹⁴K. O. Klepp, W. Sparlinek, and H. Boller, *J. Alloy Comp.* **238**, 1 (1996).
¹⁵K. Kihou, T. Saito, S. Ishida, M. Nakajima, Y. Tomioka, H. Fukazawa, Y. Kohori, T. Ito, S. Uchida, A. Iyo, C. Lee, and H. Eisaki, *J. Phys. Soc. Jpn.* **79**, 124713 (2010).
¹⁶G. A. Fatseas and J. B. Goodenough, *J. Solid State Chem.* **41**, 1 (1980).
¹⁷V. Ksenofontov, G. Wortmann, S. A. Medvedev, V. Tsurkan, J. Deisenhofer, A. Loidl, and C. Felser, *Phys. Rev. B* **84**, 180508(R) (2011).
¹⁸W. Li, C. Setty, X. H. Chen, and J. Hu, *arXiv:1202.4016v1*.
¹⁹J. Rodríguez-Carvajal, *Physica B* **192**, 55 (1993).
²⁰A. S. Wills, *Physica B* **276–278**, 680 (2000).
²¹J. M. Caron, J. R. Neilson, D. C. Miller, K. Arpino, A. Llobet, and T. M. McQueen, *Phys. Rev. B* **85**, 180405(R) (2012).
²²F. Ye, S. Chi, W. Bao, X. F. Wang, J. J. Ying, X. H. Chen, H. D. Wang, C. H. Dong, and M. H. Fang, *Phys. Rev. Lett.* **107**, 137003 (2011).
²³M. D. Johannes and I. I. Mazin, *Phys. Rev. B* **79**, 220510(R) (2009).
²⁴Y. Z. Zhang, I. Opahle, H. O. Jeschke, and R. Valentí, *Phys. Rev. B* **81**, 094505 (2010).
²⁵J. Zhao, W. Ratcliff, J. W. Lynn, G. F. Chen, J. L. Luo, N. L. Wang, J. Hu, and P. Dai, *Phys. Rev. B* **78**, 140504(R) (2008).
²⁶S. X. Chi, J. A. Rodriguez-Rivera, J. W. Lynn, C. L. Zhang, D. Phelan, D. K. Singh, R. Paul, and P. C. Dai, *Phys. Rev. B* **84**, 214407 (2011).
²⁷M. Wintenberger, G. André, M. Perrin, C. Garcin, and P. Imbert, *J. Magn. Magn. Mater.* **87**, 123 (1990).
²⁸T. Shimojima, K. Ishizaka, Y. Ishida, N. Katayama, K. Ohgushi, T. Kiss, M. Okawa, T. Togashi, X. Y. Wang, C. T. Chen, S. Watanabe, R. Kadota, T. Oguchi, A. Chainani, and S. Shin, *Phys. Rev. Lett.* **104**, 057002 (2010).
²⁹Y. Zhang, C. He, Z. R. Ye, J. Jiang, F. Chen, M. Xu, Q. Q. Ge, B. P. Xie, J. Wei, M. Aeschlimann, X. Y. Cui, M. Shi, J. P. Hu, and D. L. Feng, *Phys. Rev. B* **85**, 085121 (2012).